NeuroImage: Clinical 28 (2020) 102485

Contents lists available at ScienceDirect

NeuroImage: Clinical

journal homepage: www.elsevier.com/locate/ynicl

Patient, interrupted: MEG oscillation dynamics reveal temporal dysconnectivity in schizophrenia

Golnoush Alamian [a,*], Annalisa Pascarella [b], Tarek Lajnef [a], Laura Knight [c], James Walters [d], Krish D. Singh [c], Karim Jerbi [a,e,f,g,h]

[a] CoCo Lab, Department of Psychology, Université de Montréal, Canada
[b] Italian National Research Council, Rome, Italy
[c] CUBRIC, School of Psychology, College of Biomedical and Life Sciences, Cardiff University, UK
[d] MRC Centre for Neuropsychiatric Genetics and Genomics, Division of Psychological Medicine and Clinical Neurosciences, School of Medicine, College of Biomedical and Life Sciences, Cardiff University, UK
[e] MEG Center, University of Montreal, Canada
[f] UNIQUE Centre (Unifying AI and Neuroscience – Québec), Quebec, Canada
[g] Mila (Quebec AI Institute), Montreal, QC, Canada
[h] Centre de recherche de l'Institut universitaire en santé mentale de Montréal, Montreal, QC, Canada

ARTICLE INFO

Keywords:
Schizophrenia
Magnetoencephalography
Resting-state
Oscillations
Long-range-temporal-correlations
Machine-learning

ABSTRACT

Current theories of schizophrenia emphasize the role of altered information integration as the core dysfunction of this illness. While ample neuroimaging evidence for such accounts comes from investigations of spatial connectivity, understanding temporal disruptions is important to fully capture the essence of dysconnectivity in schizophrenia. Recent electrophysiology studies suggest that long-range temporal correlation (LRTC) in the amplitude dynamics of neural oscillations captures the integrity of transferred information in the healthy brain.

Thus, in this study, 25 schizophrenia patients and 25 controls (8 females/group) were recorded during two five-minutes of resting-state magnetoencephalography (once with eyes-open and once with eyes-closed). We used source-level analyses to investigate temporal dysconnectivity in patients by characterizing LRTCs across cortical and sub-cortical brain regions. In addition to standard statistical assessments, we applied a machine learning framework using support vector machine to evaluate the discriminative power of LRTCs in identifying patients from healthy controls.

We found that neural oscillations in schizophrenia patients were characterized by reduced signal memory and higher variability across time, as evidenced by cortical and subcortical attenuations of LRTCs in the alpha and beta frequency bands. Support vector machine significantly classified participants using LRTCs in key limbic and paralimbic brain areas, with decoding accuracy reaching 82%. Importantly, these brain regions belong to networks that are highly relevant to the symptomology of schizophrenia. These findings thus posit temporal dysconnectivity as a hallmark of altered information processing in schizophrenia, and help advance our understanding of this pathology.

1. Introduction

Schizophrenia is a debilitating disorder that is accompanied with severe cognitive, behavioral and functional impairments. Worldwide, ~21 million people suffer from psychotic illnesses yet, progress in understanding the pathophysiological mechanisms that underlie the symptoms of schizophrenia is relatively slow. For over 20 years, it has been suggested that dysconnectivity [*disconnection syndrome* (Friston and Frith, 1995; Weinberger et al., 1992) or *cognitive dysmetria* (Andreasen et al., 1998)], at the anatomical and functional levels, is the core dysfunction that underlines schizophrenia clinical symptoms (Friston et al., 2016).

Abbreviations: ASRM, Altman self-rating mania scale; BDI, Beck's depression inventory; LRTCs, Long-range-temporal-correlations; MEG, Magnetoencephalography; SANS, Scale for the assessment of negative symptoms; SAPS, Scale for the assessment of positive symptoms; SVM, Support vector machine.

* Corresponding author at: Université de Montréal, Department of Psychology, Marie-Victorin Pavilion, 90 ave Vincent-D'Indy, Montreal, QC H2V 2S9, Canada.
E-mail address: golnoush.alamian@umontreal.ca (G. Alamian).

https://doi.org/10.1016/j.nicl.2020.102485
Received 24 April 2020; Received in revised form 22 October 2020; Accepted 24 October 2020
Available online 5 November 2020

The idea of neural dysconnectivity (i.e. the failure of functional integration in the brain) relies on the assumption that disorganization is a key characteristic of schizophrenia. According to this theory, schizophrenia is marked by patterns of symptoms involving errors in predictive coding (leading to delusions and hallucinations), lack of language and thought organization, and, in some cases, motor disorganization. Neural dysconnectivity is thought to arise from aberrant synaptic plasticity, which has been attributed in part to abnormal modulation of N-methyl-D-aspartate (NMDA) receptors by neurotransmitters such as serotonin, dopamine and acetylcholine (Stephan et al., 2009). A recent study (Shaw et al., 2019) has shown that this atypical functioning of NMDA receptors is linked to altered gamma-band oscillations in schizophrenia. Moreover, it has been proposed that these abnormal neural connections occur within (and in-between) distinct brain regions (Yeganeh-Doost et al. 2011), and thereby lead to clusters of cognitive, affective and motor symptoms.

Functional magnetic resonance imaging (fMRI) (e.g., Alderson-Day et al., 2015; Karbasforoushan and Woodward, 2012; Narr and Leaver, 2015; Ramani, 2015; Rotarska-Jagiela et al., 2010; Yu et al., 2013) and electrophysiological studies (e.g., Ioannides et al., 2004; Sponheim et al., 1994; Uhlhaas and Singer, 2010) have probed structural and functional alterations among schizophrenia patients and have found significant and consistent differences in terms of the physical properties and connectivity patterns of their neural signal compared to controls (multimodal reviews: Alamian et al., 2017; Ćurčić-Blake et al., 2016; Pettersson-Yeo et al., 2011). Among others, some of the most commonly reported differences occur within the frontal cortices, within the thalamo-cortical pathway and between dorso-lateral prefrontal areas and amygdala (Alamian et al., 2017; Anticevic et al., 2013). While the input from fMRI has been crucial in understanding the anatomical (spatial) disruptions and task-related changes occurring in schizophrenia, the picture remains unclear about how neural dysconnectivity occurs at the fast temporal scale of neural communication. Specifically, while details on alterations of the anatomical connections between brain areas among schizophrenia patients have been reported (e.g., Cheung et al., 2008; Wagner et al., 2015) there remains an important gap in understanding how the integrity of the neural signal is changed over time, across multi-scaled windows. This type of evidence is key for understanding whether proper information integration has taken place (Henry et al., 2019; Hirvonen et al., 2017; Houck et al., 2016).

In recent years, there has been an increasing interest in investigating the temporal dynamics of neural oscillation amplitudes (Brookes et al., 2015; Cetin et al., 2016; Sanfratello et al., 2019). An approach for quantifying the properties of rhythmic brain activity is by exploring long-range temporal correlation (LRTC) in the amplitude dynamics of different frequency bands (Linkenkaer-Hansen et al., 2001; Nikulin et al., 2012; Palva et al., 2013). One way to measure LRTCs is by applying Detrended Fluctuation Analysis (DFA) on either the raw electrophysiological signal, or on the envelope (i.e. amplitude) of a given frequency band, using a sliding window of a given length (Kantelhardt et al., 2001; Peng et al., 1995). The LRTC metric quantifies the self-similarity of a signal across time. Its presence is an indication that electrophysiological signal decays slowly over time, and it is thought to speak of the temporal integrity of transferred information (Linkenkaer-Hansen et al., 2001). Interestingly, the strength of oscillatory LRTCs have been found to be highly heritable (~60%, Linkenkaer-Hansen et al. 2007) and, importantly, to be altered by disease, such as psychosis (Fernández et al., 2013).

To date, a few studies have evaluated LRTCs using DFA on resting-state EEG signal in schizophrenia. These papers showed that, while the overall temporal structure of the neural signal was maintained over time for both schizophrenia and healthy controls, it was more random in schizophrenia. Specifically, LRTCs were attenuated in the beta-band (Sun et al., 2014a, 2014b; Moran et al., 2019; Nikulin et al., 2012) and alpha-band oscillatory envelopes (Nikulin et al., 2012). The present study is based on the premise that LRTCs provide an efficient marker of altered information integration over time in schizophrenia. We propose that measuring LRTCs in cortical and subcortical brain areas, with the high temporal and spatial resolution of source-space magnetoencephalography (MEG), could provide evidence for the dysconnectivity theory of schizophrenia from a temporal point of view.

The goals of this study were to investigate how intrinsic neuromagnetic LRTCs differ among schizophrenia patients compared to healthy controls across cortical and subcortical brain areas. Moreover, we measured the relevance of these alterations in their ability to discriminate schizophrenia patients from healthy controls using a machine-learning framework. We hypothesized that the temporal properties of neural dynamics are affected by the illness and that, consequently, LRTCs as measured by DFA would be significantly diminished among schizophrenia patients compared to controls in both cortical and subcortical brain regions.

2. Materials and methods

Data collection was conducted at the Cardiff University Brain Research Imaging Centre (CUBRIC) in Wales, U.K., while the following analyses were conducted at the University of Montreal (Q.C., Canada). Ethics approval for the collection of data was obtained according to the guidelines of the NHS ethics Board in the U.K, the Cardiff University School of Psychology Ethics Board (EC.12.07.03.3164), and the Ethics Research Committee of the University of Montréal (CERAS-2018-19-069-D).

2.1. Participants

Neuroimaging and behavioural data of 26 schizophrenia patients and 28 healthy controls were collected. Control participants were neurologically and psychology healthy, and matched patients on age and gender. Patients were recruited through the Cognition and Psychosis study (i.e., from the Schizophrenia Working Group of the Psychiatric Genomics Consortium; details of the case sample recruitment and procedures are provided in (Lynham et al., 2018)), while controls were primarily recruited through ads using the Cardiff University Noticeboard and opportunistically from CUBRIC, Cardiff University. One patient was excluded due to the quality of their recording, and three controls were excluded due to the lack of a complete set of recording conditions. The final sample size included 25 schizophrenia patients and 25 controls.

Diagnosis confirmation was obtained for patients through the Schedule for Clinical Assessment in Neuropsychiatry (SCAN) interview. For both groups, participants were included in the study if they were between the ages of 16–75, had English as their first language, and normal or corrected vision. Controls were excluded if they had any history of neuropsychiatric disorders as measured by the MINI International Neuropsychiatric Interview (Sheehan et al., 1998). Participants were excluded if they had a history of drug or alcohol abuse, a diagnosis of epilepsy, head injury or stroke, metal present in their bodies or the use of mood stabilizing drugs. All participants were asked to refrain from the use of alcohol and drugs two days prior to testing.

Note that the sample size for this study was calculated taking into account the fact that we planned to use a machine learning framework. Based on the literature (i.e. multiple studies using machine learning to classify schizophrenia and controls), we expected classification decoding accuracies to roughly lie between 70 and 75%. Assuming a binomial cumulative distribution of the decoding error, and a p-value threshold of 0.001, the number of samples corresponding to a significant classification of 70 or 75% is 40 or 60 respectively (Combrisson and Jerbi, 2015). Our sample size of 50 participants fits within this interval.

2.2. Demographic and clinical data

Demographic information about each participant was collected,

including their age, gender, depression score on the Beck Depression Inventory – II (BDI-II (Beck et al., 1996)), and mania score on the Altman Self-Rating Mania Scale (ASRM (Altman et al., 1997)). In addition, for the patient group, scores on the Scale of the Assessment of Positive Symptoms (SAPS) and the Scale of the Assessment of Negative Symptoms (SANS) (Kay et al., 1987) were derived from the psychosis-subsection of the MINI International Neuropsychiatric Interview. Finally, information on antipsychotic doses were obtained and standardized using olanzapine equivalents (Gardner et al., 2010). The data was anonymized such that no identifiable information of participants was associated with their data nor subsequent analyses. Table 1 summarizes the demographic information of each subject group and average clinical scores on the BDI, ASRM, SANS, SAPS and medication dosage.

Aside for BDI-II scores (independent *t*-test, $t(46) = 4.94$, $p = 0.000011$), no significant group differences were observed. According to their scores on the BDI-II, schizophrenia patients presented on average with mild-depression, compared to controls who showed negligible signs of depression. In terms of ASRM scores, neither group showed any symptom that could correlate with mania. Finally, in terms of scores on the SANS and SAPS, patients generally appeared asymptomatic.

2.3. MEG and MRI experimental designs

Two five-minute resting-state MEG scans were recorded in each participant, once with eyes-closed and once with eyes-open, with a 275-channel (first-order gradiometers) CTF machine located at the CUBRIC in Wales, U.K. During the eyes-open recording, participants were instructed to fixate a red square projected in front of them. During both resting-state conditions, participants let their mind wander for the duration of the recordings. Reference channels were placed at fixed distances from the nasion, the left and right pre-auricular points. In addition, five electrodes were placed above and below the center of the left eye, under the left and the right temple and behind the left ear, to record eye movements/potential artifacts (Messaritaki et al., 2017). The raw MEG signal was recorded at a frequency sampling of 1200 Hz. In addition to the MEG data acquisition, an anatomical-T1 MRI scan was acquired for all participants to help with the MEG source reconstruction.

2.4. Data preprocessing and MEG source reconstruction

An in-house open-source python pipeline NeuroPycon (Meunier et al., 2020) was used for the preprocessing and source-reconstruction analysis. The continuous raw data was filtered with a zero-phase bandpass using a finite impulse response filtering (FIR 1, order = 3) between 0.1 Hz and 150 Hz, and a Hamming window. The default values for lower and upper transition bandwidths and filter length were used. The data was down-sampled from 1200 Hz to 600 Hz. Independent component analysis (ICA) was then used to remove blinks, eyes movements, heartbeat, and external artefacts from the MEG signal using the routine provided by the MNE-python package (Gramfort et al., 2013; Hyvarinen, 1999).

The anatomical MRI information of each participant was segmented with the FreeSurfer software package (Fischl, 2012) to generate an anatomical source-space that included both the cortical surface and the subcortical regions modelled as volumes. Given that each participant had different source-space dimensions, we next morphed and projected individual source spaces onto *fsaverage* (standardized space) of FreeSurfer (Greve et al., 2013). The mixed source space obtained in this manner consisted of 8196 nodes on the cortical surface, where each voxel was 5 mm apart from one another. For subcortical structures, we applied a region-of-interest (ROI) transformation and extracted the following volumes using FreeSurfer: Amygdala, Caudate, Hippocampus, Thalamus and Cerebellum. On average, these regions contained 27, 51, 73, 130 and 875 voxels, respectively.

The lead field matrix was computed using the single layer model boundary element method implemented in MNE-python (Gramfort et al., 2013). Finally, the inverse solution was computed using the inverse pipeline provided by NeuroPycon (Meunier et al., 2020) where we chose the weighted Minimum Norm Estimate (Dale and Sereno, 1993; Hämäläinen and Ilmoniemi, 1994; Hincapié et al., 2016), implemented in the MNE-python package (Gramfort et al., 2013; Hyvarinen, 1999). The dipoles of the cortical source-space were constrained to have an orientation normal to the surface, while the dipoles of the subcortical volumes were left with free orientation. In total, we extracted 8196 time-series at the cortical level, and 3 time-series per source in subcortical regions.

2.5. Measuring LRTC using DFA

To quantify LRTCs in the structure of the amplitudes of each frequency band, we used a standard procedure based on Detrended Fluctuation Analysis (DFA) (Kantelhardt et al., 2001; Peng et al., 1995), in line with previous research (Linkenkaer-Hansen et al., 2001; Nikulin et al., 2012; Nikulin and Brismar, 2005).

Briefly, DFA measures the fluctuation of linearly detrended signal as a function of a sliding time-window. The DFA scaling exponent reflects the slope of this fluctuation function, and is often referred to as the self-similarity parameter (Lux and Marchesi, 1999). It can take on a value between 0 and 1, where a value between 0 and 0.5 represents negative temporal correlation (i.e. anti-persistence of the signal in time), 0.5 represents a random (uncorrelated) signal, and a value between 0.5 and 1 represents a positive temporal correlation (persistence of the signal in time) (Hardstone et al., 2012). Simply put, in a persistent signal, large fluctuations are likely to be followed by large fluctuations and small energy fluctuations are likely to be followed by small energy fluctuations. Conversely, in an anti-persistent signal (negative correlation) large fluctuations are likely to be followed by small fluctuations and small fluctuations are likely to be followed by large fluctuations. In other words, if the scaling (DFA) exponent decreases from a value close to 1 down to a value closer to 0.5, then the temporal correlations are considered to be less persistent in time (i.e. they decay faster in time).

In order to obtain a measure of LRTCs in the MEG signal, instantaneous amplitude of the MEG signals was computed in the delta (1–4 Hz), theta (4–7), alpha (8–13 Hz), beta (15–25 Hz), and gamma (30–60 Hz) frequency bands. To this end, the raw MEG signal was first filtered using a finite impulse response filtering (FIR1, order = 3), and then we computed the Hilbert transform (Foster et al., 2016; Le Van Quyen et al., 2001). Next, DFA values were calculated for each of the 8196 nodes of the cortex for the length of the recording as described in (Linkenkaer-Hansen et al., 2001; Peng et al., 1995). In terms of deep structures, DFA was computed for each of the 3 time-series of each source, and then averaged across the 3 in order to obtain a single time-series per deep source. For the present study, DFA was used to analyze the decay of temporal auto-correlations, for each eyes-open and eyes-closed

Table 1
Average demographic and clinical information of participants. The ± symbol indicates the standard deviations. ASRM = Altman Self-Rating Mania Scale, BDI = Beck's depression inventory, F = females, M = males, SANS = Scale for the assessment of negative symptoms, SAPS = Scale for the assessment of positive symptoms, Schizophrenia = SZ.

	Age	Gender	Medication dose	BDI-II	ASRM	SANS	SAPS
Controls	44.04 (±9.20)	17 M; 8F	n/a	4.50(±4.67)	3.25(±3.54)	n/a	n/a
SZ Patients	44.96 (±8.55)	17 M; 8F	13.03(±13.80)	14.83(±9.11)	3.46(±2.40)	3.96(±2.92)	3.72(±4.00)

condition, in the time range of 5–33 s (or 3000–20000 samples) over consecutive windows for the full 5 min of MEG recording.

2.6. Statistics and machine-learning analyses

2.6.1. Conventional statistics and correlation analyses

Group statistical analyses were conducted between schizophrenia patients and matched-controls to test for group-level differences in (a) LRTC scaling exponents (calculated on spectral amplitudes) (b) spectral amplitudes (amplitude envelope of band-passed signals), and (c) demographic and clinical data. To do so, we used non-parametric statistical tests (two-tailed, unpaired, pseudo t-tests), corrected with maximum statistics using permutations ($n = 1000$, $p < 0.001$) (Nichols and Holmes, 2001; Pantazis et al., 2005). Two-tailed, paired, t-tests were also used (within each group) to test for changes between the eyes-open and eyes-closed conditions (both for spectral amplitude and LRTC exponents). Moreover, Pearson correlation with False Discovery Rate (FDR) correction (Genovese et al., 2002) were used to explore the relationship between cortex-level LRTCs and scores on the BDI, ASRM, SANS and SAPS, as well as to investigate the link between age, gender and medication dosage and values of LRTCs. This was also repeated for correlations between amplitude and clinical scores. FDR correction (Benjamini-Hochberg) was applied to each p-value (computed for each of the 8196 nodes), and Bonferroni correction was then applied to account for all the frequency bands (5) and correlational analyses (7) to achieve a significance threshold of $p < 0.05$ corrected.

2.6.2. Machine learning analyses

MEG signal classification was conducted using a support vector machine model and a stratified 10-fold cross-validation scheme to evaluate the discriminative power of LRTC in objectively classifying patients and controls. To do so, the DFA exponent features for each source were split into 10 folds while respecting the balance between the two classes (schizophrenia, controls). Then, the classifier was trained on the data from nine of the folds and tested on the remaining fold (test set). The classification performance was assessed using the decoding accuracy (DA) on the test set (i.e., percentage of correctly classified participants across the total number of participants in the test set). This operation was iteratively repeated until all folds were used as test sets. The mean DA was used as the classification performance metric. In order to infer the statistical significance of the obtained DAs, permutations tests were applied to derive a statistical threshold as described in (Combrisson and Jerbi, 2015). This method consists of generating a null-distribution of DAs obtained by running multiple instances of the classification ($n = 1000$), each time randomly shuffling class labels. Maximum statistics were applied across all sources in order to control for multiple comparisons (Nichols and Holmes, 2001; Pantazis et al., 2005). The same procedure was also applied to the comparison of spectral amplitudes between the groups. Finally, we used Visbrain for the visualizations of all cortical results (Combrisson et al., 2019).

2.7. Data availability

The code used throughout this study relies on open tools available to the community, including primarily the following python tools (NeuroPycon, MNE, visbrain) which can be downloaded from Github. The functions for DFA and the SVM classifiers trained in this study can be made available upon reasonable request.

3. Results

The following sections describe the results obtained with the eyes-closed resting-state MEG protocol. The summary of the results obtained in the eyes-open condition are provided in the supplementary material and are summarized at the end of the Results section.

3.1. Group comparisons of LRTCs

Fig. 1 shows the results of group-averaged LRTCs in cortical source-space in the schizophrenia patient group and the control group, for each frequency band. Overall, LRTCs were attenuated in patients, compared to controls, across the cortex in the theta, alpha and beta frequency bands. Interestingly, in the delta and gamma frequency bands (1st and last row of Fig. 1), certain areas showed LRTCs to be enhanced in patients compared to controls. These differences were however non-significant when using conventional t-tests and corrected for multiple-comparison ($p > 0.05$ for two-tailed tests). In Fig. 1, the t-values reflect both the magnitude of the effect and the direction of the group differences in terms of LRTC values, with the negative (blue) t-values showing brain areas where patients have reduced LRTC values compared to controls, and the positive (red) t-values showing brain areas where patients have increased LRTC values compared to controls. By contrast, when applying a machine-learning approach to test for out-of-sample generalization in the same data, we found that LRTCs in the alpha and beta bands in multiple brain regions led to statistically significant classification of the two subject groups with up to 82% decoding accuracy (Fig. 2, max statistics correction, $p < 0.005$). More specifically, using source-space alpha-band LRTCs as a decoding feature led to statistically significant discrimination of schizophrenia and controls in the precentral, central and postcentral gyri and sulci, the right frontal gyrus, the left temporal gyrus, the bilateral temporal poles and sulci and the medical parts of parahippocampal gyri (Fig. 2a). Meanwhile, using source-space beta-band LRTCs as a decoding feature let to statistically significant classification of schizophrenia patients and controls in the bilateral orbitofrontal cortices, the right parahippocampal gyrus, bilateral orbital gyri, bilateral anterior cingulate gyri and sulci and left insular sulcus (Fig. 2b). To illustrate how the classifier was able to successfully separate patients from controls, we computed individual LRTC values, averaged in each subject across all brain sites that exhibited successful decoding. These were computed separately for alpha and beta-band LRTCs and are presented in a scatter plot (Fig. 3a). For comparison, Fig. 3b shows individual alpha and beta amplitude values averaged over the same brain regions. As can be seen, amplitude values in the alpha and beta bands in the same nodes do not allow for a clear separation of the groups. This provides further qualitative confirmation that the LRTC-based classification results are not driven by changes in amplitude. Fig. 4 shows the classification results of schizophrenia and controls using the estimated alpha-band and beta-band LRTCs from the estimated time-series in deep structures. In terms of subcortical structures, statistically significant classification (max statistics correction, $p < 0.001$) of schizophrenia versus controls was obtained with alpha-band LRTC features from the combination of the left and right amygdala, the left hippocampus, the left thalamus and the combination of the left and right cerebellum (Fig. 4a). In the beta frequency band, the right amygdala, the combination of the left and right amygdala, the combination of the left and right caudate, and the combination of the left and right thalamus were able to statistically significantly (max statistics correction, $p < 0.001$) discriminate the two groups with a success rate of up to 74% (Fig. 4b). No other frequency band's LRTCs led to significant classification.

3.2. Group comparisons of spectral amplitude

To appreciate the putative value of LRTC features, we also computed the same contrasts and classification using, the more standard, spectral amplitude as feature. Fig. 5 shows both increased and decreased oscillatory amplitudes among schizophrenia patients compared to controls. Conventional t-tests of the amplitude did not yield any significant group differences after multiple comparison correction in any of the frequency bands ($p > 0.05$ for two-tailed tests). Nevertheless, Fig. 5 shows the t-values to indicate the magnitude and direction of the group differences in terms of amplitude magnitude, with the negative (blue) t-values

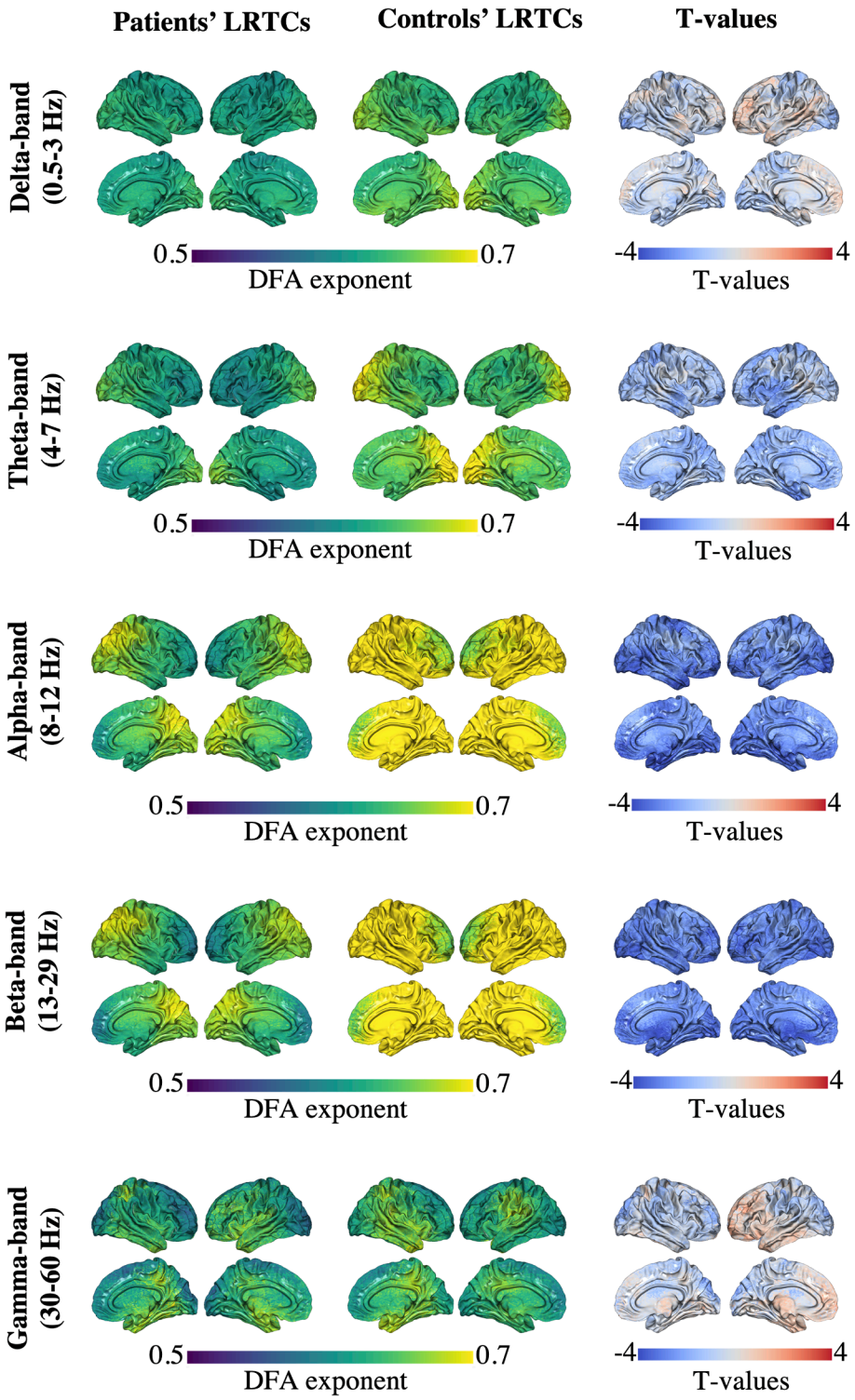

Fig. 1. Source-level results of LRTCs of schizophrenia patients and controls. Columns 1 and 2 show mean LRTC values for each group. Column 3 shows the T-values of the unpaired t-tests (non-significant). DFA = detrended fluctuation analysis, LRTCs = long-range temporal correlations.

showing brain areas where patients have reduced amplitude compared to controls, and the positive (red) t-values showing brain areas where patients have increased amplitude compared to controls. This was also the case when using SVM classification in all frequency bands, except for the gamma-band oscillatory amplitude, which led to a statistically significant classification (Fig. 6). In particular, gamma-band oscillations led to statistically significant discrimination in the orbital sulci and gyri, parahippocampal gyri, temporal poles, left superior temporal sulcus, and left temporal gyrus, with patients showing higher spectral amplitude levels in these given brain structures. The highest discrimination occurred in the left temporal pole with a decoding accuracy of 84% (Fig. 6, max statistics correction, $p < 0.005$).

Fig. 7 shows the classification results of schizophrenia and controls using the alpha (Fig. 7a), beta (Fig. 7b) and gamma (Fig. 7c) bands oscillatory amplitude in the deep structures. In terms of subcortical structures, the gamma-band amplitude of the left caudate significantly

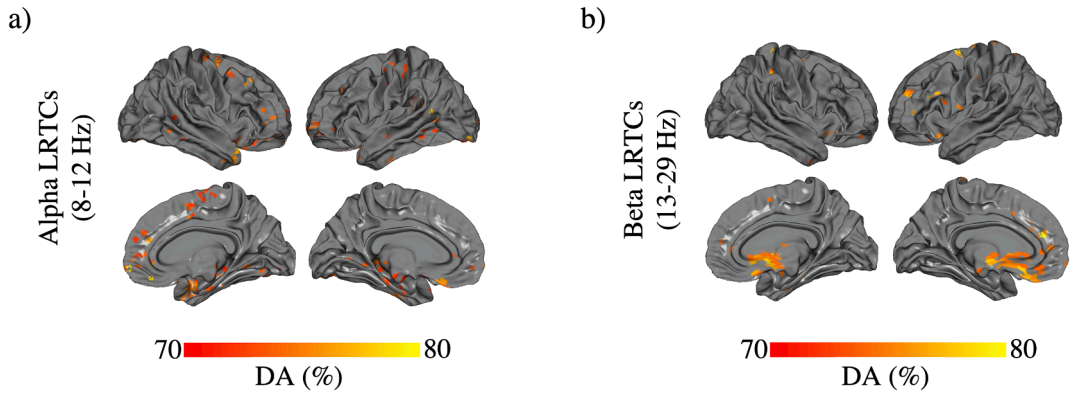

Fig. 2. Classification of schizophrenia patients and healthy controls in the cortex. SVM used alpha (a) and beta (b) DFA exponents (LRTCs) as discriminant features at the cortical level. The images are thresholded at statistically significant decoding accuracy ($p < 0.005$, permutation tests and max statistics correction). DA = decoding accuracy, DFA = detrended fluctuation analysis, LRTCs = long-range temporal correlations, SVM = support vector machine.

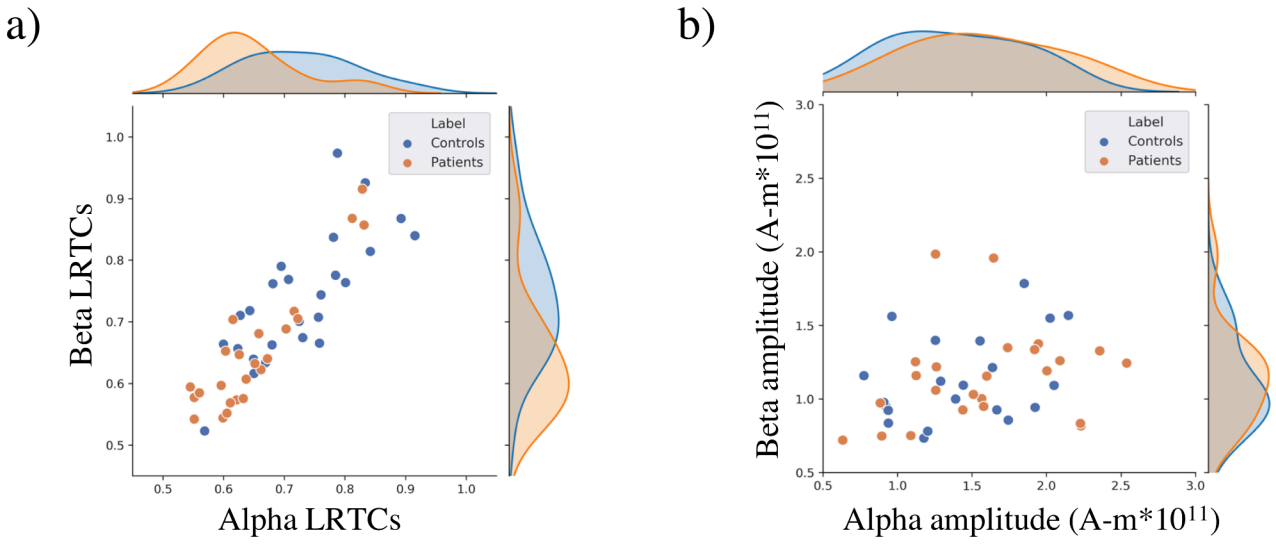

Fig. 3. Scatter plot visualization of individual LRTC and amplitude values in brain regions with statistically significant classification. (a) illustrates individual LRTC values, averaged across all the nodes that showed statistically significant patient vs controls decoding in the alpha and beta frequency bands (n = 50). (b) illustrates individual amplitude values ($A-m*10^{-11}$) in the alpha and beta in the same brain regions (n = 46, data from 4 outliers were excluded due to amplitude values > 5 std above the mean).

decoded the two groups, as well as the amygdala (using the left, right, and both hemispheres), hippocampus (using the left and both hemispheres) and cerebellum (using both hemispheres) (72–79%, max statistics correction, $p < 0.001$, Fig. 7c).

3.3. Correlations with clinical and demographic information

The investigation of the potential correlations between LRTCs and demographic and clinical information yielded no significant results across the five frequency bands. However, the analysis of correlation between amplitude of different frequency bands and schizophrenia patients' negative symptom scores yielded a highly statistically significant result in the theta band (Fig. 8). Specifically, spectral amplitude of the delta (Fig. 8a) and theta band (Fig. 8b) correlated positively with schizophrenia patients' scores on the SANS clinical scale (max correlation $r = 0.81$, $p < 0.05$, corrected for multiple comparisons)

3.4. Summary of eyes-open resting-state condition results

Similarly to the eyes-closed resting-state condition, LRTCs appeared to be attenuated in schizophrenia patients in the theta, alpha and beta frequency bands, and slightly enhanced in the gamma band, compared to controls (Supplementary Fig. 1). With our machine-learning approach, patients and controls were again significantly classified using LRTCs in the alpha and beta frequency bands with up to 79% decoding accuracy (max statistics correction, $p < 0.005$, Fig. 9a). Specifically, using source-space alpha-band LRTCs as a decoding feature led to statistically significant discrimination of schizophrenia and controls in the postcentral gyri and sulci, and in the superior temporal gyri and sulci (bilaterally). Moreover, using source-space beta-band LRTCs as a decoding feature let to statistically significant classification of schizophrenia patients and controls in the right precentral gyrus and sulcus, right central sulcus, right postcentral gyrus, right superior-frontal gyrus and paracentral lobules. In terms of subcortical structures, SVM significantly classified (max statistics correct, $p < 0.001$) the two groups using alpha-band LRTCs in the left amygdala, left hippocampus and the combination of the left and right hippocampi (Fig. 9c and Supplementary Fig. 2).

The examination of spectral amplitude in the eyes-open condition showed increased oscillatory amplitude in patients in the delta, theta and gamma bands, while a trend of decreased amplitude was seen in the alpha and beta bands (Supplementary Fig. 3). Statistical analyses of the amplitude did not reveal any significant group differences in any of the frequency bands. However, machine-learning classification of

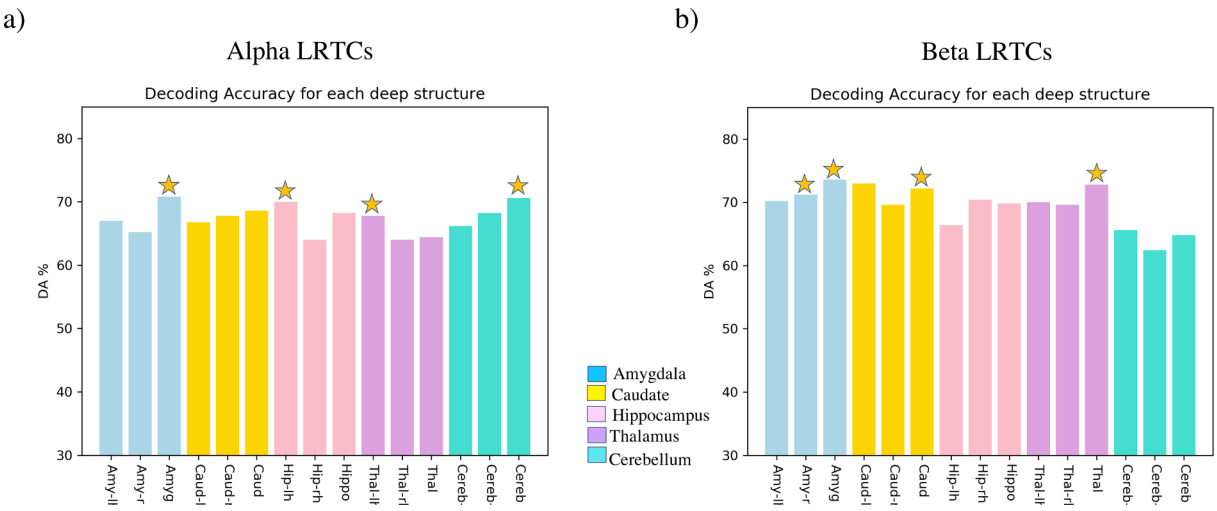

Fig. 4. Classification of schizophrenia patients and healthy controls at the sub-cortical level. SVM used alpha (a) and beta (b) DFA exponents (LRTC) as discriminant features computed in deep structure ROIs. Statistically significant decoded ROIs are indicated with a star ($p < 0.001$). The suffix "-lh" indicates left hemisphere, "-rh" indicates right hemisphere, and no suffix reflects classification using both left and right hemispheres. Amy = amygdala, Caud = caudate, Cereb = cerebellum, DA = decoding accuracy, DFA = detrended fluctuation analysis, Hipp = hippocampus, LRTCs = long-range temporal correlations, SVM = support vector machine, Thal = thalamus.

schizophrenia patients and controls using spectral amplitude yielded significant discriminatory patterns in the delta, theta, beta and gamma bands (Fig. 8b). In particular, statistically significant classification of groups were observed in delta-band oscillations in the left postcentral and parieto-occipital sulci and the right temporal pole; in theta-band oscillations in the left parieto-occipital sulcus; in the beta-band in the right orbital and precuneus gyri and temporal pole; and the most significant decoding accuracies were observed in the gamma band, in the left rectus gyrus (88%, max statistics correction, $p < 0.005$), along with the right orbital gyrus, orbital sulci and left parahippocampal gyrus. Supplementary Fig. 4 shows the classification results of schizophrenia and controls using the alpha, beta and gamma bands oscillatory amplitude in the deep structures. Beta-band amplitude of the right hippocampus significantly decoded the two groups (74%, max statistics correction, $p < 0.001$). In terms of gamma oscillations, significant classification (74–78%, max statistics correction, $p < 0.001$, Fig. 9d and Supplementary Fig. 4) of patients and controls were observed in the amygdala (using the left and both hemispheres), the hippocampus (using the left, right, and both hemispheres) and the cerebellum (using the left, right, and both hemispheres).

Finally, in terms of correlation analyses between LRTCs/spectral amplitude and patients' clinical scores, significant correlational results between theta-amplitude and SANS scores were observed, similar to those in the eye closed condition (max correlation $r = 0.81$, $p < 0.05$, corrected for multiple comparison, Fig. 9e).

3.5. Comparison of eyes-closed and eyes-open resting-state conditions

Within-group, statistical comparisons of the eyes-open and eyes-closed conditions revealed a cortex-wide attenuation of LRTC values in the alpha and beta band for controls in the eyes-open condition, compared to eyes-closed (paired t-tests, max stat correction, 1000 permutations, $p < 0.05$). However, in the case of schizophrenia patients, this LRTC difference between eyes open and closed was not statistically significant, although it did appear that LRTC values were higher in the eyes-closed than in the eyes-open condition.

In terms of amplitudes differences, paired t-tests showed that amplitude magnitudes of the alpha-band were substantially higher in the eyes-closed condition than the eyes-open condition for both schizophrenia patients and healthy controls, particularly in the temporal and visual cortices, as expected. This difference was even bigger in schizophrenia patients, as the occipital lobe differences were statistically significant after multiple-comparison correction ($p < 0.05$, max stat, 1000 permutations).

4. Discussion

Although widely studied, the neural mechanisms underpinning the symptomology of schizophrenia are still somewhat elusive. Given that correct diagnosis and early treatment is crucial for medication adherence and good prognosis, the clinical research community has focused on identifying characteristics that are unique to this pathology. To address this, the leading theory of neural dysconnectivity has been explored extensively in the spatial domain, but very little has been discussed in terms of *temporal* dysconnectivity in schizophrenia. The aim of this study was to explore whether schizophrenia-specific differences exist within the temporal structure of neural oscillations, during resting-state, using MEG measurements to probe both cortical and subcortical brain regions. Our results show that this is indeed the case. This finding corroborates and extends previous studies that have observed both healthy and pathological brain-signals to exhibit DFA exponents that were between 0.5 and 1 (Berthouze et al., 2010; Fedele et al., 2016; Linkenkaer-Hansen et al., 2004, 2001; Nikulin and Brismar, 2005, 2004). While the resting neural system exhibited temporal persistence (scaling exponent above 0.5), indicating that the structure of the brain signal was maintained through time for both groups, the weaker exponents found in schizophrenia patients suggest a loss in persistence (or memory) in the signal. This drop from values close to 1 towards 0.5 is reflective of near-uncorrelated signals (Linkenkaer-Hansen et al., 2001; Peng et al., 1995) and has often been thought to be indicative of diminished regularity (Beggs and Timme, 2012) and a change in the neuronal excitability-inhibitory balance (La Rocca et al., 2018; Poil et al., 2012). This might be due to changes in NMDA-receptor conductance, which in-turn would increase the variability of a signal, decrease the stability of the signal's memory, and increase the chance for a change in state (e.g. order to disorder) (Loh et al., 2007; Rolls et al., 2008).

Furthermore, the attenuated temporal auto-correlations in schizophrenia were confined to the alpha and beta envelopes in distinct cortical and subcortical areas. Indeed, single-feature SVM classification was able to successfully differentiate the two groups with up to 82% decoding accuracy, solely based on the measure of LRTCs. In the alpha-

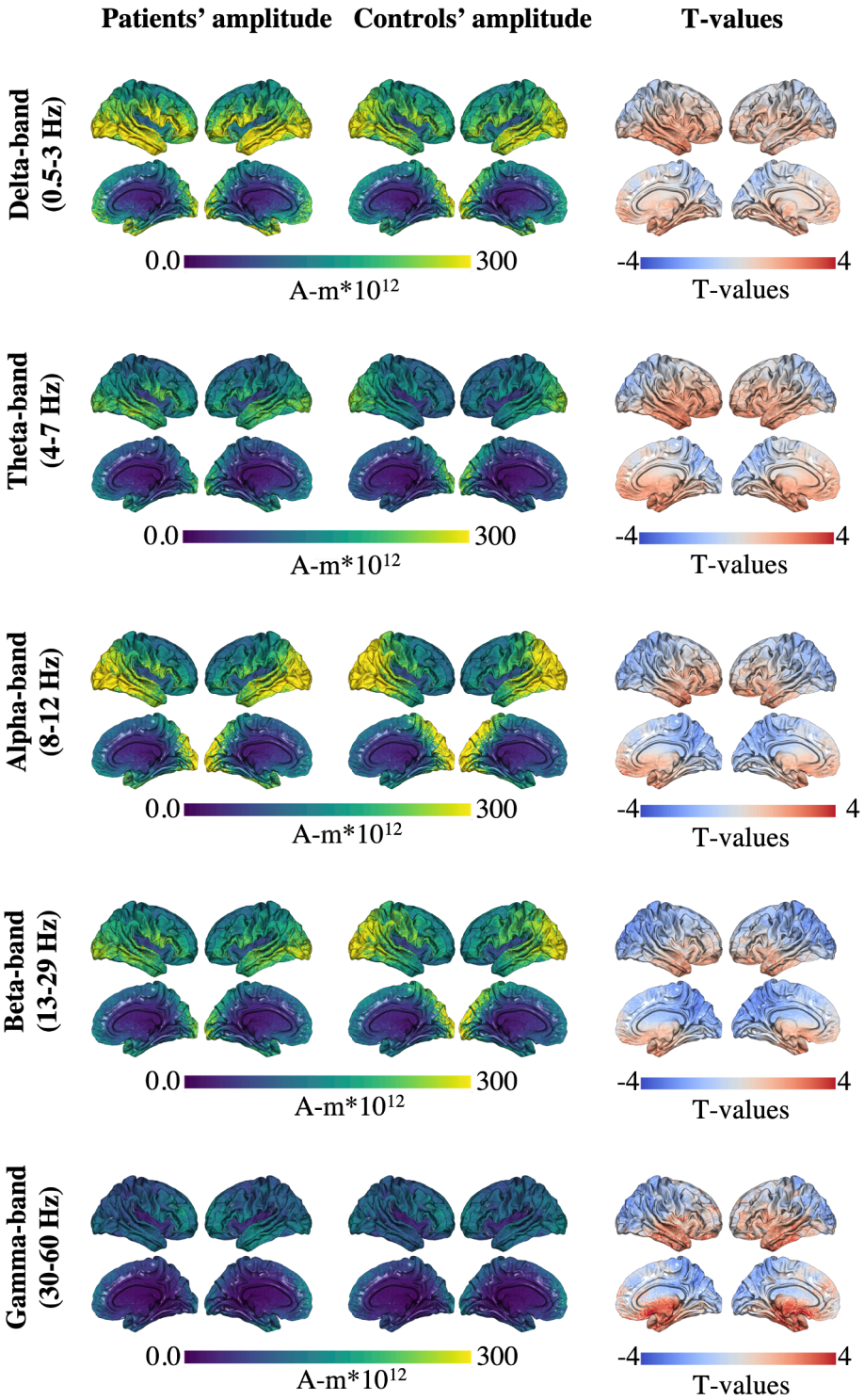

Fig. 5. Source-level results of spectral amplitude of patients and controls. Columns 1 and 2 show averaged amplitude values for each group at each node (A−m $*10^{-12}$). Column 3 shows T-values based on the unpaired t-tests (non-significant).

band, the brain areas that significantly contributed to the classification of patients and controls included the pre and post central gyri and sulci, temporal poles, temporal gyrus and the parahippocampal gyri. In the beta-band, these regions included the orbitofrontal cortices, the anterior cingulate gyri and sulci, the left insula and the right parahippocampal gyrus. Structural (Ohi et al., 2016) and functional (Wang et al., 2015) alterations of the temporal lobe have been previously highlighted (e.g., reduced grey matter volume). Moreover, the paralimbic areas mentioned above seem to be involved in hallucinations (Silbersweig et al., 1995), as well as the cognitive hypofunctioning in schizophrenia that occurs due to early neurodevelopmental deficits (Isomura et al., 2017; Liao et al., 2015; Xu et al., 2017).

Importantly, the unpreceded analyses of LRTC alterations in subcortical substructures reported here provides the first evidence that LRTC values computed on alpha and beta band-limited envelopes in deep structures are altered in schizophrenia, to the extent that they allow for robust discrimination between patients and controls in an out-of-sample generalization context (cross-validated machine learning

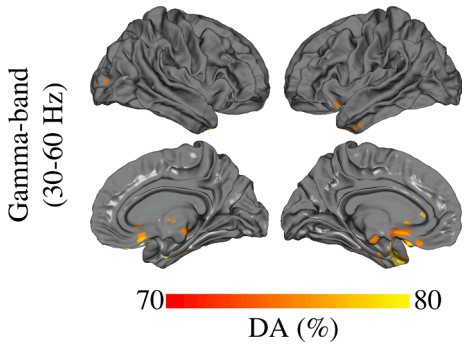

Fig. 6. Significant classification of schizophrenia patients and healthy controls based on amplitude. SVM in the spectral amplitude of gamma at the cortical-level significantly classified groups. The images are thresholded at statistically significant decoding accuracy ($p < 0.005$, permutation tests and max statistics correction). DA = decoding accuracy, SVM = support vector machine.

framework). More specifically, statistically significant predictions (schizophrenia patient vs healthy control) was possible using alpha-band LRTC in the amygdala, left hippocampus, left thalamus and cerebellum, and using beta-band LRTC in the amygdala, caudate and thalamus. Our control analyses of spectral amplitude showed that the observed LRTC alterations were not confounded by differences in oscillatory power. Moreover, the lack of statistical difference in age or gender suggests that the results were not mediated by these demographic parameters. Despite being a recognized challenge, MEG studies increasingly report activity in subcortical structure (Rivolta et al., 2015; Youssofzadeh et al., 2018) including the amygdala (Lu et al., 2012; Nugent et al., 2015). Alterations in subcortical structures in schizophrenia have been reported in the literature; It is well-known that schizophrenia is associated with pathological changes in thalamic activity (Giraldo-Chica and Woodward, 2016; Woodward et al., 2012). Specifically, the thalamo-cortical dysconnectivity has been pinned as a key player in the cognitive symptoms of patients e.g. (Chen et al., 2019; Uhlhaas et al., 2013). In addition, a number of fMRI resting-studies studies have discussed the implication of the hippocampus, amygdala, caudate and cerebellum in the pathophysiology of schizophrenia. Of particular interest, the observed beta-band LRTC alterations in the amygdala is consistent with previously reported amygdala changes at the structural (Rajarethinam et al., 2001; Velakoulis et al., 2006) and functional/connectivity levels (Mukherjee et al., 2013). This limbic area is implicated in social cognition (Adolphs, 2002) and damage to it can lead to aberrant social judgement, similar to what is seen in schizophrenia.

With respect to spectral amplitude, our findings confirm previous studies that observed increased power in resting-state MEG gamma-band oscillations in schizophrenia patients (Andreou et al., 2015,

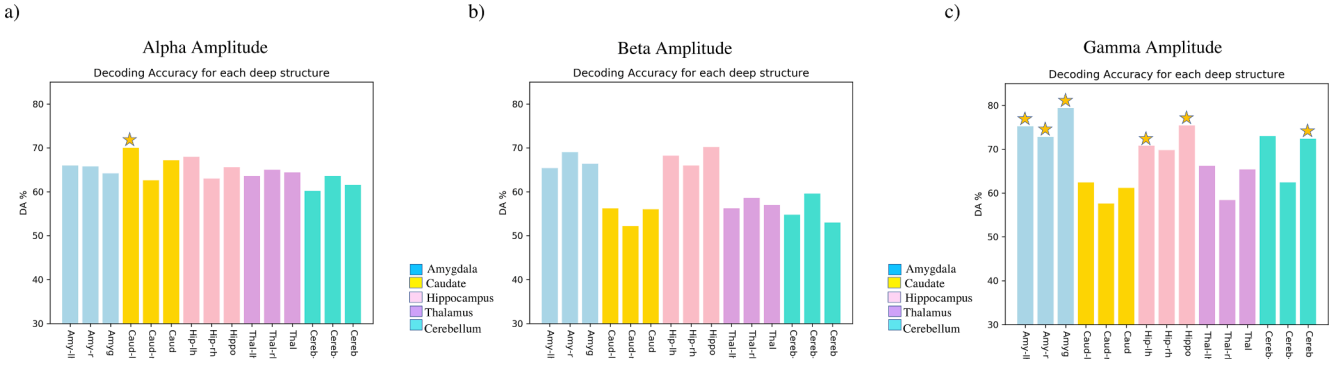

Fig. 7. Classification of schizophrenia patients and controls based on spectral amplitude at the sub-cortical level. SVM, with a 10-fold cross validation, applied max statistics and 1000 permutations classified groups. Statistically significant decoded ROIs are indicated with a star ($p < 0.001$). The suffix "-lh" indicates left hemisphere, "-rh" indicates right hemisphere, and no suffix reflects classification using both left and right hemispheres. Amy = amygdala, Caud = caudate, Cereb = cerebellum, DA = decoding accuracy, Hipp = hippocampus, LRTCs = long-range temporal correlations, ROI = region of interest, SVM = support vector machine, Thal = thalamus.

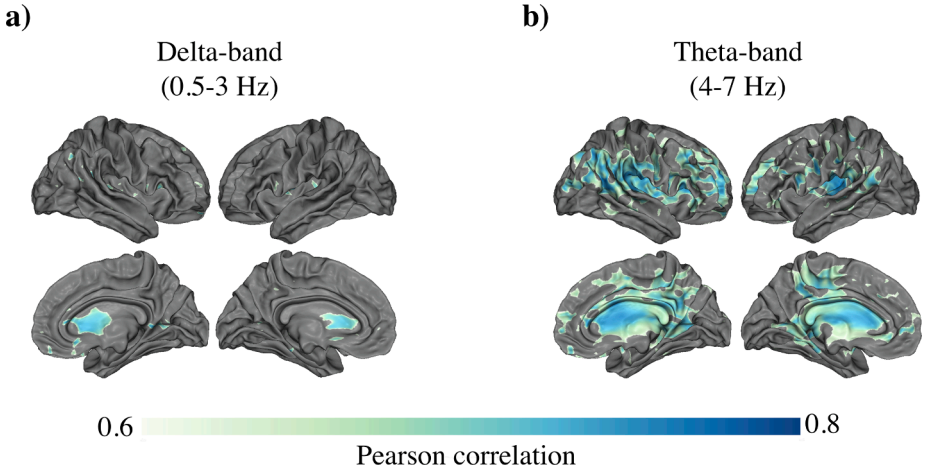

Fig. 8. Correlation between spectral amplitude and patients' symptoms. Pearson correlation between (a) delta-band amplitude and patients' scores on the scale for the assessment of negative symptoms (SANS), and (b) between theta-band amplitude and SANS scores. The maps are thresholded at a p-value of 0.05, corrected for multiple comparisons.

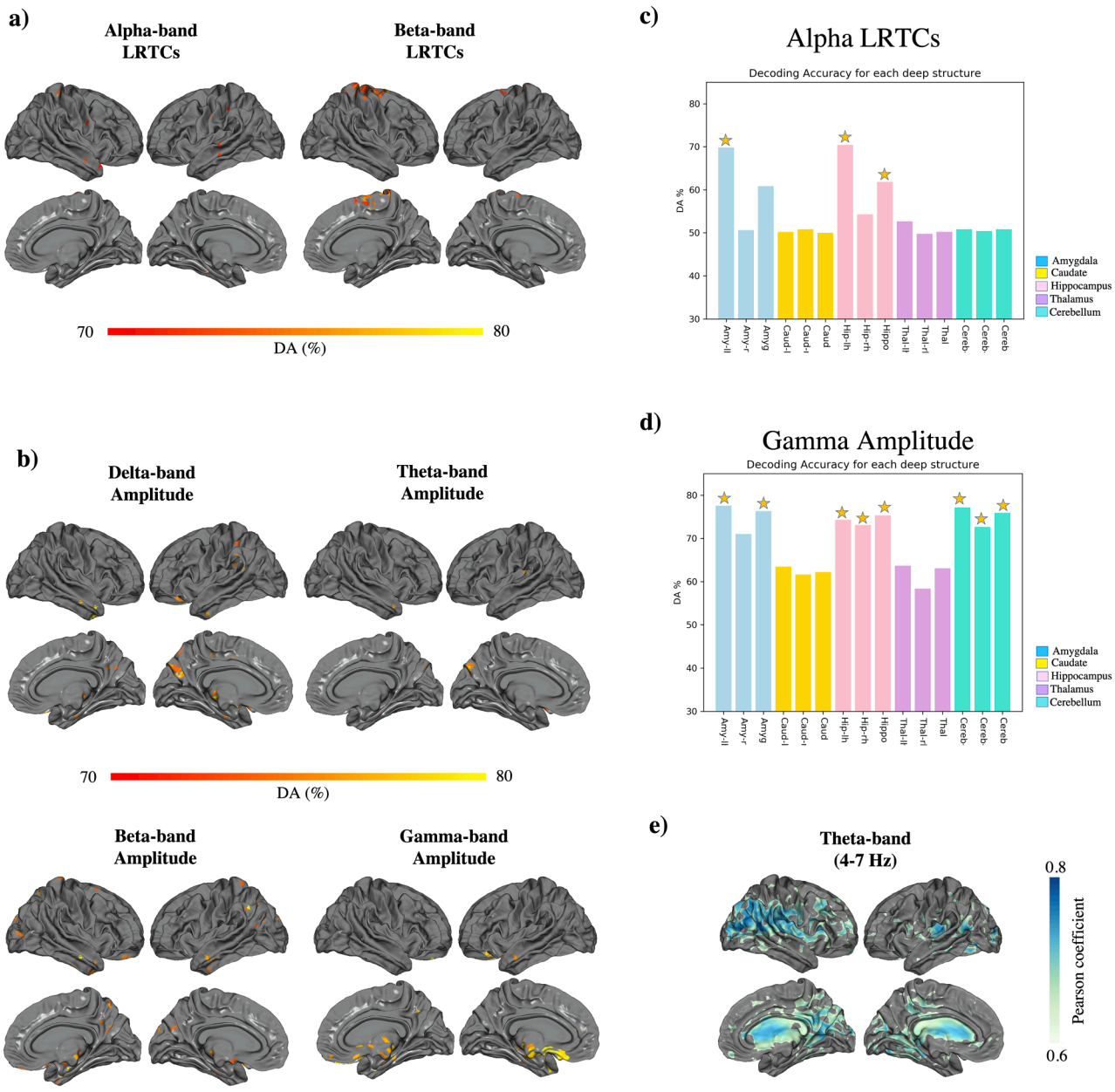

Fig. 9. Summary of main results of the eyes-open condition. (a) and (c) illustrate statistically significant classification of schizophrenia patients and controls based on LRTCs and amplitude, respectively, at the cortical level ($p < 0.005$, permutation tests and max statistics correction). (b) and (d) illustrate classification of patients and controls based on LRTCs and amplitude, respectively, at the subcortical level. Statistically significant decoded ROIs are indicated with a star ($p < 0.001$). The suffix "-lh" indicates left hemisphere, "-rh" indicates right hemisphere, and no suffix reflects classification using both left and right hemispheres. (e) Pearson correlation between theta-band amplitude and patients' scores on the SANS ($p < 0.05$, corrected for multiple comparisons). Amy = amygdala, Caud = caudate, Cereb = cerebellum, DA = decoding accuracy, Hipp = hippocampus, LRTCs = long-range temporal correlations, ROI = region of interest, SANS = scale for the assessment of negative symptoms, Thal = thalamus.

2014; Di Lorenzo et al., 2015; Gandal et al., 2012; Mitra et al., 2015; Northoff and Duncan, 2016; Venables et al., 2009; White and Siegel, 2016). SVM was able to successfully classify the two participant groups based on gamma-band amplitude in the orbital cortex, parahippocampal gyri, temporal cortex, amygdala, hippocampus and cerebellum. However, no significant amplitude differences were observed in the alpha and beta frequency bands, where the prominent LRTC changes were found. This rules-out any speculations that the LRTC alterations in schizophrenia are driven by the effect or magnitude of spectral amplitude. It should be noted that, although ocular movement-related artefacts were removed using ICA, it is possible that some of the gamma-band amplitude differences, and thereby the gamma amplitude decoding results, could in part be due to uncaptured eye motion in patients.

Correlational analyses looking at LRTCs and patients' clinical information yielded no significant results. In terms of amplitude however, we observed a strong positive correlation between the theta-band amplitude and SANS score. The brain regions involved in this finding were comprised of the parieto-temporal lobes, bilaterally. This result is in-line with previous studies that have observed enhanced resting low-frequency activity (Chen et al., 2016; Fehr et al., 2003, 2001; Sperling et al., 2002; Wienbruch et al., 2003), as well as positive correlations between low frequency oscillations and patients' negative symptoms (Chen et al., 2016; Fehr et al., 2003; Jandl et al., 2005; Venables et al., 2009; review: Boutros et al., 2014). Unlike the recent publication by (Zeev-Wolf et al., 2018), however, correlations between alpha or beta-band power and patients' symptoms scores were not significant. This

could be due to the way the authors divided their patient group into high and low negative scores, and high and low positive scores, while we did not perform such separation of our participants, particularly since our patient group was fairly asymptomatic. It is also possible that this difference is due to our smaller sample size, or our statistical thresholds and the strict correction that we applied for our comparisons.

Our robust and statistically significant machine-learning findings highlight the potential of using scaling dynamics as an early biomarker of schizophrenia. During typical development, LRTCs appear to increase and strengthen during the transition from childhood to adolescence (Smit et al., 2011). This phase is also a critical period during which psychopathologies typically arise (van den Heuvel and Kahn, 2011). Thus, we hypothesized that diminished LRTCs in patho-relevant areas could potentially reflect neural alterations during brain maturation among schizophrenia patients that parallel those of excess synaptic-pruning, which lead to reduced gray matter volume (Uhlhaas, 2011). Indeed, both reduced gray matter volume (Witthaus et al., 2009) and white matter (Quan et al., 2013) have been reported in the same brain regions where we found diminished LRTCs (e.g., inferior frontal gyrus, which is thought to relate to core executive functions, such as inhibitory response) (Swick et al., 2008). Future longitudinal research that includes MEG recordings in large cohorts of individuals at-risk of developing psychosis is recommended to further the findings of the present study.

Comparison of the eyes-open and eyes-closed conditions revealed that LRTC values were overall higher in the eyes-closed than in the eyes-open condition, particularly for healthy controls and less so for schizophrenia patients. This result is opposite to the one reported by (Sun et al., 2014a, 2014b), who did not find significant differences between eyes open and closed in healthy controls' LRTCs. With respect to schizophrenia patients, their LRTCs values were more similar, perhaps because the reported LRTCs values were lower to begin with (and already close to the lower-bound value of 0.5) compared to controls. Interestingly, our LRTC findings in the beta-band (eyes-open condition) were consistent with that of a recent EEG paper by (Moran et al., 2019). While it is unclear why substantial differences in LRTCs exist in the eyes-open and eyes-closed conditions, we hypothesize that differential neural mechanisms are at work, and thus bring about differences in the temporal structure of neural activity. It is tempting to hypothesize that when healthy participants close their eyes, they reach a more relaxed state, which in turn allows for better signal memory and autocorrelation in the system. Conversely, this state is perhaps harder to attain for schizophrenia patients who exhibit more neuronal excitability (scaling exponents closer to 0.5) with their eyes closed. This may partly be in line with the prevalence of sleep-related disorder among schizophrenia patients (Monti and Monti, 2005). It is also noteworthy that the type of instructions given to participants prior to resting-state recordings can influence their neural dynamics (Benjamin et al., 2010; Kawagoe et al., 2018). In the present study, participants let their mind wander during the eyes-open and eyes-closed recordings, thus allowing for a more natural baseline state of rest, compared to potentially more effortful instructions (e.g., "try not to think of anything", Kawagoe et al., 2018).

Taken together, the results of this study characterize, for the first time, temporal dysconnectivity in schizophrenia patients at both the cortical and subcortical levels using MEG. In addition, the machine-learning findings provide good evidence for the use of resting-state LRTCs in alpha and beta frequency bands to confidently discriminate patients from controls.

5. Conclusion

In summary, this study shows that models such as the *cognitive dysmetria* and the *disconnection syndrome* can be probed, confirmed and extended using electrophysiological measures of resting neural dynamics (Smart et al., 2015). Indeed, the observed attenuation in temporal autocorrelation in the envelopes of the alpha and beta-band oscillations among schizophrenia patients supports the theory of dysconnectivity from a *temporal* angle. Taken together, this new approach for the quantification of (temporal) dysconnectivity could lead to new venues of research, early diagnosis and treatment for schizophrenia patients.

Declaration of Competing Interest

The authors declare that they have no known competing financial interests or personal relationships that could have appeared to influence the work reported in this paper.

Acknowledgements

We would like to acknowledge Dmitrii Altukov and Thomas Thiery for their contribution to this work.

Funding

This research was supported in part by the FRQNT Strategic Clusters Program [grant number 2020-RS4-265502 – Centre UNIQUE – Union Neurosciences & Artificial Intelligence – Quebec]. The scanning was supported by CUBRIC and the Schools of Psychology and Medicine at Cardiff University, together with the MRC/EPSRC funded UK MEG Partnership Grant [grant number MR/K005464/1]. Golnoush Alamian was supported by the Fonds de Recherche du Québec en Santé. Tarek Lajnef was supported by the postdoctoral fellowship from IVADO. Karim Jerbi was supported by funding from the Canada Research Chairs program and a Discovery Grant [grant number RGPIN-2015-04854] from NSERC (Canada), a New Investigators Award from FRQNT [grant number 2018-NC-206005] and an IVADO-Apogée fundamental research project grant.

Appendix A. Supplementary data

Supplementary data to this article can be found online at https://doi.org/10.1016/j.nicl.2020.102485.

References

Adolphs, R., 2002. Neural systems for recognizing emotion. Curr. Opin. Neurobiol. 12, 169–177. https://doi.org/10.1016/S0959-4388(02)00301-X.

Alamian, G., Hincapié, A.-S., Pascarella, A., Thiery, T., Combrisson, E., Saive, A.-L., Martel, V., Althukov, D., Haesebaert, F., Jerbi, K., 2017. Measuring alterations in oscillatory brain networks in schizophrenia with resting-state MEG: State-of-the-art and methodological challenges. Clin. Neurophysiol. 128, 1719–1736. https://doi.org/10.1016/j.clinph.2017.06.246.

Alderson-Day, B., McCarthy-Jones, S., Fernyhough, C., 2015. Hearing voices in the resting brain: A review of intrinsic functional connectivity research on auditory verbal hallucinations. Neurosci. Biobehav. Rev. 55, 78–87. https://doi.org/10.1016/j.neubiorev.2015.04.016.

Altman, E.G., Hedeker, D., Peterson, J.L., Davis, J.M., 1997. The Altman Self-Rating Mania Scale. Biol. Psychiatry 42, 948–955. https://doi.org/10.1016/S0006-3223(96)00548-3.

Andreasen, N.C., Paradiso, S., O'Leary, D.S., 1998. Cognitive dysmetria as an integrative theory of schizophrenia: a dysfunction in cortical-subcortical-cerebellar circuitry? Schizophr. Bull. 24, 203–218.

Andreou, C., Faber, P.L., Leicht, G., Schoettle, D., Polomac, N., Hanganu-Opatz, I.L., Lehmann, D., Mulert, C., 2014. Resting-state connectivity in the prodromal phase of schizophrenia: Insights from EEG microstates. Schizophr. Res. 152, 513–520. https://doi.org/10.1016/j.schres.2013.12.008.

Andreou, C., Nolte, G., Leicht, G., Polomac, N., Hanganu-Opatz, I.L., Lambert, M., Engel, A.K., Mulert, C., 2015. Increased Resting-State Gamma-Band Connectivity in First-Episode Schizophrenia. Schizophr. Bull. 41, 930–939. https://doi.org/10.1093/schbul/sbu121.

Anticevic, A., Brumbaugh, M.S., Winkler, A.M., Lombardo, L.E., Barrett, J., Corlett, P.R., Kober, H., Gruber, J., Repovs, G., Cole, M.W., Krystal, J.H., Pearlson, G.D., Glahn, D. C., 2013. Global prefrontal and fronto-amygdala dysconnectivity in bipolar I disorder with psychosis history. Biol. Psychiatry 73, 565–573. https://doi.org/10.1016/j.biopsych.2012.07.031.

Beck, A.T., Steer, R.A., Brown, G.K., 1996. Manual for the Beck Depression Inventory-II. Psychological Corporation, San Antonio, TX, USA.

Beggs, J.M., Timme, N., 2012. Being critical of criticality in the brain. Front. Physiol. doi: 10.3389/fphys.2012.00163.

Benjamin, C., Lieberman, D.A., Changl, M., Ofen, N., Whitfield-Gabrieli, S., Gabrieli, J.D. E., Gaab, N., 2010. The influence of rest period instructions on the default mode network. Front. Hum. Neurosci. 4 https://doi.org/10.3389/fnhum.2010.00218.

Berthouze, L., James, L.M., Farmer, S.F., 2010. Human EEG shows long-range temporal correlations of oscillation amplitude in Theta, Alpha and Beta bands across a wide age range. Clin. Neurophysiol. Off. J. Int. Fed. Clin. Neurophysiol. 121, 1187–1197. https://doi.org/10.1016/j.clinph.2010.02.163.

Boutros, N.N., Mucci, A., Diwadkar, V., Tandon, R., 2014. Negative Symptoms in Schizophrenia: A Comprehensive Review of Electrophysiological Investigations. Clin. Schizophr. Relat. Psychoses 28–35.

Brookes, M.J., Hall, E.L., Robson, S.E., Price, D., Palaniyappan, L., Liddle, E.B., Liddle, P. F., Robinson, S.E., Morris, P.G., 2015. Complexity measures in magnetoencephalography: measuring "disorder" in schizophrenia. PLoS One 10, e0120991. https://doi.org/10.1371/journal.pone.0120991.

Cetin, M.S., Houck, J.M., Rashid, B., Agacoglu, O., Stephen, J.M., Sui, J., Canive, J., Mayer, A., Aine, C., Bustillo, J.R., Calhoun, V.D., 2016. Multimodal Classification of Schizophrenia Patients with MEG and fMRI Data Using Static and Dynamic Connectivity Measures. Front. Neurosci. 10, 466. https://doi.org/10.3389/fnins.2016.00466.

Chen, P., Ye, E., Jin, X., Zhu, Y., Wang, L., 2019. Association between Thalamocortical Functional Connectivity Abnormalities and Cognitive Deficits in Schizophrenia. Sci. Rep. 9 https://doi.org/10.1038/s41598-019-39367-z.

Chen, Y.-H., Stone-Howell, B., Edgar, J.C., Huang, M., Wootton, C., Hunter, M.A., Lu, B. Y., Sadek, J.R., Miller, G.A., Cañive, J.M., 2016. Frontal slow-wave activity as a predictor of negative symptoms, cognition and functional capacity in schizophrenia. Br. J. Psychiatry 208.

Cheung, V., Cheung, C., McAlonan, G.M., Deng, Y., Wong, J.G., Yip, L., Tai, K.S., Khong, P.L., Sham, P., Chua, S.E., 2008. A diffusion tensor imaging study of structural dysconnectivity in never-medicated, first-episode schizophrenia. Psychol. Med. 38, 877–885. https://doi.org/10.1017/S0033291707001808.

Combrisson, E., Jerbi, K., 2015. Exceeding chance level by chance: The caveat of theoretical chance levels in brain signal classification and statistical assessment of decoding accuracy. J. Neurosci. Methods 250, 126–136. https://doi.org/10.1016/J.JNEUMETH.2015.01.010.

Combrisson, E., Vallat, R., O'Reilly, C., Jas, M., Pascarella, A., Saive, A., Thiery, T., Meunier, D., Altukhov, D., Lajnef, T., Ruby, P., Guillot, A., Jerbi, K., 2019. Visbrain: A Multi-Purpose GPU-Accelerated Open-Source Suite for Multimodal Brain Data Visualization. Front. Neuroinform. 13 https://doi.org/10.3389/fninf.2019.00014.

Ćurčić-Blake, B., Ford, J., Hubl, D., Orlov, N.D., Sommer, I.E., Waters, F., Allen, P., Jardri, R., Woodruff, P.W., Olivier, D., Mulert, C., Woodward, T.S., Aleman, A., 2016. Interaction of language, auditory and memory brain networks in auditory verbal hallucinations. Prog. Neurobiol. https://doi.org/10.1016/j.pneurobio.2016.11.002.

Dale, A.M., Sereno, M.I., 1993. Improved Localization of Cortical Activity by Combining EEG and MEG with MRI Cortical Surfarce Reconstruction: A Linear Approach. J. Cogn. Neurosicence 5, 162–176.

Di Lorenzo, G., Daverio, A., Ferrentino, F., Santarnecchi, E., Ciabattini, F., Monaco, L., Lisi, G., Barone, Y., Di Lorenzo, C., Niolu, C., Seri, S., Siracusano, A., 2015. Altered resting-state EEG source functional connectivity in schizophrenia: the effect of illness duration. Front. Hum. Neurosci. 9, 234. https://doi.org/10.3389/fnhum.2015.00234.

Fedele, T., Blagovechtchenski, E., Nazarova, M., Iscan, Z., Moiseeva, V., Nikulin, V.V., 2016. Long-Range Temporal Correlations in the amplitude of alpha oscillations predict and reflect strength of intracortical facilitation: Combined TMS and EEG study. Neuroscience 331, 109–119. https://doi.org/10.1016/j.neuroscience.2016.06.015.

Fehr, T., Kissler, J., Moratti, S., Wienbruch, C., Rockstroh, B., Elbert, T., 2001. Source distribution of neuromagnetic slow waves and MEG-delta activity in schizophrenic patients. Biol. Psychiatry 50, 108–116. https://doi.org/10.1016/S0006-3223(01)01122-2.

Fehr, T., Kissler, J., Wienbruch, C., Moratti, S., Elbert, T., Watzl, H., Rockstroh, B., 2003. Source distribution of neuromagnetic slow-wave activity in schizophrenic patients—effects of activation. Schizophr. Res. 63, 63–71. https://doi.org/10.1016/S0920-9964(02)00213-X.

Fernández, A., Gómez, C., Hornero, R., López-Ibor, J.J., 2013. Complexity and schizophrenia. Prog. Neuro-Psychopharmacology Biol. Psychiatry 45, 267–276. https://doi.org/10.1016/j.pnpbp.2012.03.015.

Fischl, B., 2012. FreeSurfer. Neuroimage. https://doi.org/10.1016/j.neuroimage.2012.01.021.

Foster, B.L., He, B.J., Honey, C.J., Jerbi, K., Maier, A., Saalmann, Y.B., 2016. Spontaneous Neural Dynamics and Multi-scale Network Organization. Front. Syst. Neurosci. 10, 7. https://doi.org/10.3389/fnsys.2016.00007.

Friston, K., Brown, H.R., Siemerkus, J., Stephan, K.E., 2016. The dysconnection hypothesis (2016). Schizophr. Res. 176, 83–94. https://doi.org/10.1016/j.schres.2016.07.014.

Friston, K.J., Frith, C.D., 1995. Schizophrenia: A disconnection syndrome? Clin. Neurosci. 3, 89–97.

Gandal, M.J., Edgar, J.C., Klook, K., Siegel, S.J., 2012. Gamma synchrony: towards a translational biomarker for the treatment-resistant symptoms of schizophrenia. Neuropharmacology 62, 1504–1518. https://doi.org/10.1016/j.neuropharm.2011.02.007.

Gardner, D., Murphy, A., O'Donnell, H., Centorrino, F., Baldessarini, R., 2010. International Consensus Study of Antipsychotic Dosing. Am J Psychiatry 167, 686–693.

Genovese, C.R., Lazar, N.A., Nichols, T., 2002. Thresholding of Statistical Maps in Functional Neuroimaging Using the False Discovery Rate. Neuroimage 15, 870–878. https://doi.org/10.1006/NIMG.2001.1037.

Giraldo-Chica, M., Woodward, N.D., 2016. Review of thalamocortical resting-state fMRI studies in schizophrenia. Schizophr. Res. https://doi.org/10.1016/j.schres.2016.08.005.

Gramfort, A., Luessi, M., Larson, E., Engemann, D.A., Strohmeier, D., Brodbeck, C., Goj, R., Jas, M., Brooks, T., Parkkonen, L., Hämäläinen, M., 2013. MEG and EEG data analysis with MNE-Python. Front. Neurosci. 7, 267. https://doi.org/10.3389/fnins.2013.00267.

Greve, D.N., Van der Haegen, L., Cai, Q., Stufflebeam, S., Sabuncu, M.R., Fischl, B., Brysbaert, M., 2013. A surface-based analysis of language lateralization and cortical asymmetry. J. Cogn. Neurosci. 25, 1477–1492. https://doi.org/10.1162/jocn_a_00405.

Hämäläinen, M.S., Ilmoniemi, R.J., 1994. Interpreting magnetic fields of the brain: minimum norm estimates. Med. Biol. Eng. Comput. 32, 35–42. https://doi.org/10.1007/BF02512476.

Hardstone, R., Poil, S.-S., Schiavone, G., Jansen, R., Nikulin, V.V., Mansvelder, H.D., Linkenkaer-Hansen, K., 2012. Detrended fluctuation analysis: a scale-free view on neuronal oscillations. Front. Physiol. 3, 450. https://doi.org/10.3389/fphys.2012.00450.

Henry, P., Coffman, B.A., Ghuman, A.S., Sejdic, E., Salisbury, D.F., 2019. Non-negative matrix factorization reveals resting-state cortical alpha network abnormalities in the first-episode schizophrenia spectrum. Biol. Psychiatry Cogn. Neurosci. Neuroimaging.

Hincapié, A.-S., Kujala, J., Mattout, Jérémie, Daligault, S., Delpuech, C., Mery, D., Cosmelli, D., Jerbi, K., 2016. Connectivity and Power Detections with Minimum Norm Estimates Require Different Regularization Parameters. Comput. Intell. Neurosci. 2016, 1–11. https://doi.org/10.1155/2016/3979547.

Hirvonen, J., Wibral, M., Palva, J.M., Singer, W., Uhlhaas, P., Palva, S., 2017. Whole-Brain Source-Reconstructed MEG-Data Reveal Reduced Long-Range Synchronization in Chronic Schizophrenia. eNeuro 4. https://doi.org/10.1523/ENEURO.0338-17.2017.

Houck, J.M., Çetin, M.S., Mayer, A.R., Bustillo, J.R., Stephen, J., Aine, C., Cañive, J., Perrone-Bizzozero, N., Thoma, R.J., Brookes, M.J., Calhoun, V.D., 2016. Magnetoencephalographic and functional MRI connectomics in schizophrenia via intra- and inter-network connectivity. Neuroimage. https://doi.org/10.1016/j.neuroimage.2016.10.011.

Hyvarinen, A., 1999. Fast and robust fixed-point algorithms for independent component analysis. IEEE Trans. Neural Networks 10, 626–634. https://doi.org/10.1109/72.761722.

Ioannides, A.A., Poghosyan, V., Dammers, J., Streit, M., 2004. Real-time neural activity and connectivity in healthy individuals and schizophrenia patients. Neuroimage 23, 473–482. https://doi.org/10.1016/j.neuroimage.2004.06.023.

Isomura, S., Hashimoto, R., Nakamura, M., Hirano, Y., Yamashita, F., Jimbo, S., Yamamori, H., Fujimoto, M., Yasuda, Y., Mears, R.P., Onitsuka, T., 2017. Altered sulcogyral patterns of orbitofrontal cortex in a large cohort of patients with schizophrenia. npj Schizophr. 3 https://doi.org/10.1038/s41537-016-0008-y.

Jandl, M., Bittner, R., Sack, A., Weber, B., Gü Nther, T., Pieschl, D., Kaschka, W.-P., Maurer, K., 2005. Changes in negative symptoms and EEG in schizophrenic patients after repetitive Transcranial Magnetic Stimulation (rTMS): an open-label pilot study. J. Neural Transm. 112, 955–967. https://doi.org/10.1007/s00702-004-0229-5.

Sun, Junfeng, Tang, Yingying, Lim, K.O., Wang, Jijun, Tong, Shanbao, Li, Hui, He, Bin, 2014a. Abnormal Dynamics of EEG Oscillations in Schizophrenia Patients on Multiple Time Scales. IEEE Trans. Biomed. Eng. 61, 1756–1764. https://doi.org/10.1109/TBME.2014.2306424.

Kantelhardt, J.W., Koscielny-Bunde, E., Rego, H.H.A., Havlin, S., Bunde, A., 2001. Detecting Long-range Correlations with Detrended Fluctuation Analysis. Phys. A Stat. Mech. its Appl. 295, 441–454. https://doi.org/10.1016/S0378-4371(01)00144-3.

Karbasforoushan, H., Woodward, N.D., 2012. Resting-state networks in schizophrenia. Curr. Top. Med. Chem. 12, 2404–2414.

Kawagoe, T., Onoda, K., Yamaguchi, S., 2018. Different pre-scanning instructions induce distinct psychological and resting brain states during functional magnetic resonance imaging. Eur. J. Neurosci. 47, 77–82. https://doi.org/10.1111/ejn.13787.

Kay, S.R., Fiszbein, A., Opler, L.A., 1987. The Positive and Negative Syndrome Scale (PANSS) for Schizophrenia. Schizophr. Bull. 13, 261–276. https://doi.org/10.1093/schbul/13.2.261.

La Rocca, D., Zilber, N., Abry, P., van Wassenhove, V., Ciuciu, P., 2018. Self-similarity and multifractality in human brain activity: a wavelet-based analysis of scale-free brain dynamics. Self-similarity multifractality Hum. brain Act. A wavelet-based Anal. scale-free brain Dyn. 315853. doi:10.1101/315853.

Le Van Quyen, M., Foucher, J., Lachaux, J.-P., Rodriguez, E., Lutz, A., Martinerie, J., Varela, F.J., 2001. Comparison of Hilbert transform and wavelet methods for the analysis of neuronal synchrony. J. Neurosci. Methods 111, 83–98. https://doi.org/10.1016/S0165-0270(01)00372-7.

Liao, J., Yan, H., Liu, Q., Yan, J., Zhang, L., Jiang, S., Zhang, X., Dong, Z., Yang, W., Cai, L., Guo, H., Wang, Y., Li, Z., Tian, L., Zhang, D., Wang, F., 2015. Reduced paralimbic system gray matter volume in schizophrenia: Correlations with clinical variables, symptomatology and cognitive function. J. Psychiatr. Res. 65, 80–86. https://doi.org/10.1016/j.jpsychires.2015.04.008.

Linkenkaer-Hansen, K., Nikouline, V.V., Palva, J.M., Ilmoniemi, R.J., 2001. Long-range temporal correlations and scaling behavior in human brain oscillations. J. Neurosci. 21, 1370–1377. https://doi.org/10.1523/JNEUROSCI.21-04-01370.2001.

Linkenkaer-Hansen, K., Nikulin, V.V., Palva, S., Ilmoniemi, R.J., Palva, J.M., 2004. Prestimulus Oscillations Enhance Psychophysical Performance in Humans. J. Neurosci. 24, 10186–10190. https://doi.org/10.1523/JNEUROSCI.2584-04.2004.

Linkenkaer-Hansen, K., Smit, D.J.A., Barkil, A., van Beijsterveldt, T.E.M., Brussaard, A.B., Boomsma, D.I., van Ooyen, A., de Geus, E.J.C., 2007. Genetic Contributions to Long-Range Temporal Correlations in Ongoing Oscillations. J. Neurosci. 27, 13882–13889. https://doi.org/10.1523/JNEUROSCI.3083-07.2007.

Loh, M., Rolls, E., Deco, G., 2007. A Dynamical Systems Hypothesis of Schizophrenia. PLOS Comput. Biol. 3, e228.

Lu, Q., Li, H., Luo, G., Wang, Y., Tang, H., Han, L., Yao, Z., 2012. Impaired prefrontal-amygdala effective connectivity is responsible for the dysfunction of emotion process in major depressive disorder: A dynamic causal modeling study on MEG. Neurosci. Lett. 523, 125–130. https://doi.org/10.1016/j.neulet.2012.06.058.

Lux, T., Marchesi, M., 1999. Scaling and criticality in a stochastic multi-agent model of a financial market. Nature 397, 498–500. https://doi.org/10.1038/17290.

Lynham, A., Hubbard, L., Tansey, K., Marian, L., Legge, S., Owen, M., Jones, I., Walters, J., 2018. Examining cognition across the bipolar/schizophrenia diagnostic spectrum. J. Psychiatry Neurosci. 43, 245–253.

Messaritaki, E., Koelewijn, L., Dima, D.C., Williams, G.M., Perry, G., Singh, K.D., 2017. Assessment and elimination of the effects of head movement on MEG resting-state measures of oscillatory brain activity. Neuroimage 159, 302–324. https://doi.org/10.1016/j.neuroimage.2017.07.038.

Meunier, D., Pascarella, A., Altukhov, D., Jas, M., Combrisson, E., Lajnef, T., Bertrand-Dubois, D., Hadid, V., Alamian, G., Alves, J., Barlaam, F., Saive, A.-L., Dehgan, A., Jerbi, K., 2020. NeuroPycon: An open-source Python toolbox for fast multi-modal and reproducible brain connectivity pipelines. Neuroimage 219, 117020. https://doi.org/10.1016/j.neuroimage.2020.117020.

Mitra, S., Nizamie, S.H., Goyal, N., Tikka, S.K., 2015. Evaluation of resting state gamma power as a response marker in schizophrenia. Psychiatry Clin. Neurosci. 69, 630–639. https://doi.org/10.1111/pcn.12301.

Monti, J.M., Monti, D., 2005. Sleep disturbance in schizophrenia. Int. Rev. Psychiatry 17, 247–253. https://doi.org/10.1080/09540260500104516.

Moran, J.K., Michail, G., Heinz, A., Keil, J., Senkowski, D., 2019. Long-Range Temporal Correlations in Resting State Beta Oscillations are Reduced in Schizophrenia. Front. Psychiatry 10. https://doi.org/10.3389/fpsyt.2019.00517.

Mukherjee, P., Whalley, H.C., McKirdy, J.W., Sprengelmeyer, R., Young, A.W., McIntosh, A.M., Lawrie, S.M., Hall, J., 2013. Altered Amygdala Connectivity Within the Social Brain in Schizophrenia. Schizophr. Bull. 40, 152–160. https://doi.org/10.1093/schbul/sbt086.

Narr, K.L., Leaver, A.M., 2015. Connectome and schizophrenia. Curr. Opin. Psychiatry 28, 229–235. https://doi.org/10.1097/YCO.0000000000000157.

Nichols, T.E., Holmes, A.P., 2001. Nonparametric Permutation Tests For Functional Neuroimaging: A Primer with Examples.

Nikulin, V.V., Brismar, T., 2005. Long-range temporal correlations in electroencephalographic oscillations: Relation to topography, frequency band, age and gender. Neuroscience 130, 549–558. https://doi.org/10.1016/j.neuroscience.2004.10.007.

Nikulin, V.V., Brismar, T., 2004. Long-range temporal correlations in alpha and beta oscillations: effect of arousal level and test-retest reliability. Clin. Neurophysiol. Off. J. Int. Fed. Clin. Neurophysiol. 115, 1896–1908. https://doi.org/10.1016/j.clinph.2004.03.019.

Nikulin, V.V., Jönsson, E.G., Brismar, T., 2012. Attenuation of long-range temporal correlations in the amplitude dynamics of alpha and beta neuronal oscillations in patients with schizophrenia. Neuroimage 61, 162–169. https://doi.org/10.1016/j.neuroimage.2012.03.008.

Northoff, G., Duncan, N.W., 2016. How do abnormalities in the brain's spontaneous activity translate into symptoms in schizophrenia? From an overview of resting state activity findings to a proposed spatiotemporal psychopathology. Prog. Neurobiol. https://doi.org/10.1016/j.pneurobio.2016.08.003.

Nugent, A.C., Robinson, S.E., Coppola, R., Furey, M.L., Zarate, C.A., 2015. Group differences in MEG-ICA derived resting state networks: Application to major depressive disorder. Neuroimage 118, 1–12. https://doi.org/10.1016/j.neuroimage.2015.05.051.

Ohi, K., Matsuda, Y., Shimada, T., Yasuyama, T., Oshima, K., Sawai, K., Kihara, H., Nitta, Y., Okubo, H., Uehara, T., Kawasaki, Y., 2016. Structural alterations of the superior temporal gyrus in schizophrenia: Detailed subregional differences. Eur. Psychiatry 35, 25–31. https://doi.org/10.1016/j.eurpsy.2016.02.002.

Palva, J.M., Zhigalov, A., Hirvonen, J., Korhonen, O., Linkenkaer-Hansen, K., Palva, S., 2013. Neuronal long-range temporal correlations and avalanche dynamics are correlated with behavioral scaling laws. Proc. Natl. Acad. Sci. U. S. A. 110, 3585–3590. https://doi.org/10.1073/pnas.1216855110.

Pantazis, D., Nichols, T.E., Baillet, S., Leahy, R.M., 2005. A comparison of random field theory and permutation methods for the statistical analysis of MEG data. Neuroimage 25, 383–394. https://doi.org/10.1016/j.neuroimage.2004.09.040.

Peng, C.K., Havlin, S., Stanley, H.E., Goldberger, A.L., 1995. Quantification of scaling exponents and crossover phenomena in nonstationary heartbeat time series. Chaos 5, 82–87. https://doi.org/10.1063/1.166141.

Pettersson-Yeo, W., Allen, P., Benetti, S., McGuire, P., Mechelli, A., 2011. Dysconnectivity in schizophrenia: Where are we now? Biobehav. Rev. Neurosci. https://doi.org/10.1016/j.neubiorev.2010.11.004.

Poil, S.-S., Hardstone, R., Mansvelder, H.D., Linkenkaer-Hansen, K., 2012. Critical-state dynamics of avalanches and oscillations jointly emerge from balanced excitation/inhibition in neuronal networks. J. Neurosci. 32, 9817–9823. https://doi.org/10.1523/JNEUROSCI.5990-11.2012.

Quan, M., Lee, S.-H., Kubicki, M., Kikinis, Z., Rathi, Y., Seidman, L.J., Mesholam-Gately, R.I., Goldstein, J.M., McCarley, R.W., Shenton, M.E., Levitt, J.J., 2013. White matter tract abnormalities between rostral middle frontal gyrus, inferior frontal gyrus and striatum in first-episode schizophrenia. Schizophr. Res. 145, 1–10. https://doi.org/10.1016/J.SCHRES.2012.11.028.

Rajarethinam, R., DeQuardo, J.R., Miedler, J., Arndt, S., Kirbat, R.A., Brunberg, J., Tandon, R., 2001. Hippocampus and amygdala in schizophrenia: Assessment of the relationship of neuroanatomy to psychopathology. Psychiatry Res. - Neuroimaging 108, 79–87. https://doi.org/10.1016/S0925-4927(01)00120-2.

Ramani, R., 2015. Connectivity. Curr. Opin. Anaesthesiol. 28, 498–504. https://doi.org/10.1097/ACO.0000000000000237.

Rivolta, D., Heidegger, T., Scheller, B., Sauer, A., Schaum, M., Birkner, K., Singer, W., Wibral, M., Uhlhaas, P.J., 2015. Ketamine Dysregulates the Amplitude and Connectivity of High-Frequency Oscillations in Cortical-Subcortical Networks in Humans: Evidence From Resting-State Magnetoencephalography-Recordings. Schizophr. Bull. 41, 1105–1114. https://doi.org/10.1093/schbul/sbv051.

Rolls, E., Loh, M., Deco, G., Winterer, G., 2008. Computational models of schizophrenia and dopamine modulation in the prefrontal cortex. Nat. Rev. Neurosci. 9, 696–709.

Rotarska-Jagiela, A., van de Ven, V., Oertel-Knöchel, V., Uhlhaas, P.J., Vogeley, K., Linden, D.E.J., 2010. Resting-state functional network correlates of psychotic symptoms in schizophrenia. Schizophr. Res. 117, 21–30. https://doi.org/10.1016/j.schres.2010.01.001.

Sanfratello, L., Houck, J.M., Calhoun, V., 2019. Dynamic functional network connectivity in schizophrenia with magnetoencephalography and functional magnetic resonance imaging: do different timescales tell a different story? Brain Connect. 9, 251–262.

Shaw, A., Knight, L., Freeman, T., Williams, G., Moran, R., Friston, K.J., Walters, J., Singh, K.D., 2019. Oscillatory, computational, and behavioral evidence for impaired GABAergic inhibition in schizophrenia. Schizophr. Bull. sbz066.

Sheehan, D. V., Lecrubier, Y., Sheehan, K.H., Amorim, P., Janavs, J., Weiller, E., Hergueta, T., Baker, R., Dunbar, G.C., 1998. The Journal of clinical psychiatry, The Journal of Clinical Psychiatry. [Physicians Postgraduate Press].

Silbersweig, D.A., Stern, E., Frith, C., Cahill, C., Holmes, A., Grootoonk, S., Seaward, J., Mc Kenna, P., Chua, S.E., Schnorr, L., Jones, T., Frackowiak, R.S.J., 1995. A functional neuroanatomy of hallucinations in schizophrenia. Nature 378, 176–179. https://doi.org/10.1038/378176a0.

Smart, O.L., Tiruvadi, V.R., Mayberg, H.S., 2015. Multimodal approaches to define network oscillations in depression. Biol. Psychiatry 77, 1061–1070. https://doi.org/10.1016/j.biopsych.2015.01.002.

Smit, D.J.A., de Geus, E.J.C., van de Nieuwenhuijzen, M.E., van Beijsterveldt, C.E.M., van Baal, G.C.M., Mansvelder, H.D., Boomsma, D.I., Linkenkaer-Hansen, K., 2011. Scale-free modulation of resting-state neuronal oscillations reflects prolonged brain maturation in humans. J. Neurosci. 31, 13128–13136. https://doi.org/10.1523/JNEUROSCI.1678-11.2011.

Sperling, W., Martus, P., Kober, H., Bleich, S., Kornhuber, J., 2002. Spontaneous, slow and fast magnetoencephalographic activity in patients with schizophrenia. Schizophr. Res. 58, 189–199. https://doi.org/10.1016/S0920-9964(02)00238-4.

Sponheim, S.R., Clementz, B.A., Iacono, W.G., Beiser, M., 1994. Resting EEG in first-episode and chronic schizophrenia. Psychophysiology 31, 37–43. https://doi.org/10.1111/j.1469-8986.1994.tb01023.x.

Stephan, K.E., Friston, K.J., Frith, C.D., 2009. Dysconnection in schizophrenia: from abnormal synaptic plasticity to failures of self-monitoring. Schizophr. Bull. 35, 509–527. https://doi.org/10.1093/schbul/sbn176.

Sun, J., Tang, Y., Lim, K.O., Wang, J., Tong, S., Li, H., He, B., 2014b. Abnormal dynamics of EEG oscillations in schizophrenia patients on multiple time scales. Biomed. Eng. IEEE Trans. https://doi.org/10.1109/TBME.2014.2306424.

Swick, D., Ashley, V., Turken, A.U., 2008. Left inferior frontal gyrus is critical for response inhibition. BMC Neurosci. 9, 102. https://doi.org/10.1186/1471-2202-9-102.

Uhlhaas, P.J., 2011. The adolescent brain: implications for the understanding, pathophysiology, and treatment of schizophrenia. Schizophr. Bull. 37, 480–483. https://doi.org/10.1093/schbul/sbr025.

Uhlhaas, P.J., Roux, F., Singer, W., 2013. Thalamocortical Synchronization and Cognition: Implications for Schizophrenia? Neuron. https://doi.org/10.1016/j.neuron.2013.02.033.

Uhlhaas, P.J., Singer, W., 2010. Abnormal neural oscillations and synchrony in schizophrenia. Nat. Rev. Neurosci. 11, 100–113. https://doi.org/10.1038/nrn2774.

van den Heuvel, M.P., Kahn, R.S., 2011. Abnormal Brain Wiring as a Pathogenetic Mechanism in Schizophrenia. Biol. Psychiatry 70, 1107–1108. https://doi.org/10.1016/j.biopsych.2011.10.020.

Velakoulis, D., Wood, S.J., Wong, M.T.H., McGorry, P.D., Yung, A., Phillips, L., Smith, D., Brewer, W., Proffitt, T., Desmond, P., Pantelis, C., 2006. Hippocampal and amygdala volumes according to psychosis stage and diagnosis: A magnetic resonance imaging study of chronic schizophrenia, first-episode psychosis, and ultra-high-risk individuals. Arch. Gen. Psychiatry 63, 139–149. https://doi.org/10.1001/archpsyc.63.2.139.

Venables, N.C., Bernat, E.M., Sponheim, S.R., 2009. Genetic and disorder-specific aspects of resting state EEG abnormalities in schizophrenia. Schizophr. Bull. 35, 826–839. https://doi.org/10.1093/schbul/sbn021.

Wagner, G., De la Cruz, F., Schachtzabel, C., Güllmar, D., Schultz, C.C., Schlösser, R.G., Bär, K.J., Koch, K., 2015. Structural and functional dysconnectivity of thefronto-thalamic system in schizophrenia: ADCM-DTI study. Cortex 66, 35–45. https://doi.org/10.1016/j.cortex.2015.02.004.

Wang, Z., Meda, S.A., Keshavan, M.S., Tamminga, C.A., Sweeney, J.A., Clementz, B.A., Schretlen, D.J., Calhoun, V.D., Lui, S., Pearlson, G.D., 2015. Large-scale fusion of gray matter and resting-state functional MRI reveals common and distinct biological markers across the psychosis spectrum in the B-SNIP cohort. Front. Psychiatry 6. https://doi.org/10.3389/fpsyt.2015.00174.

Weinberger, D.R., Berman, K.F., Suddath, R., Fuller Torrey, E., 1992. Evidence of Dysfunction of a Prefrontal-Limbic Network in Schizophrenia: A Magnetic Resonance Imaging and Regional Cerebral Blood Flow Study of Discordant Monozygotic Twins. Am J Psychiatry.

White, R.S., Siegel, S.J., 2016. Cellular and circuit models of increased resting-state network gamma activity in schizophrenia. Neuroscience 321, 66–76. https://doi.org/10.1016/j.neuroscience.2015.11.011.

Wienbruch, C., Moratti, S., Elbert, T., Vogel, U., Fehr, T., Kissler, J., Schiller, A., Rockstroh, B., 2003. Source distribution of neuromagnetic slow wave activity in schizophrenic and depressive patients. Clin. Neurophysiol. 114, 2052–2060. https://doi.org/10.1016/S1388-2457(03)00210-4.

Witthaus, H., Kaufmann, C., Bohner, G., Özgürdal, S., Gudlowski, Y., Gallinat, J., Ruhrmann, S., Brüne, M., Heinz, A., Klingebiel, R., Juckel, G., 2009. Gray matter abnormalities in subjects at ultra-high risk for schizophrenia and first-episode schizophrenic patients compared to healthy controls. Psychiatry Res. Neuroimaging 173, 163–169. https://doi.org/10.1016/J.PSCYCHRESNS.2008.08.002.

Woodward, N.D., Karbasforoushan, H., Heckers, S., 2012. Thalamocortical dysconnectivity in schizophrenia. Am. J. Psychiatry 169, 1092–1099. https://doi.org/10.1176/appi.ajp.2012.12010056.

Xu, Y., Qin, W., Zhuo, C., Xu, L., Zhu, J., Liu, X., Yu, C., 2017. Selective functional disconnection of the orbitofrontal subregions in schizophrenia. Psychol. Med. 47, 1637–1646. https://doi.org/10.1017/S0033291717000101.

Yeganeh-Doost, P., Gruber, O., Falkai, P., Schmitt, A., 2011. The role of the cerebellum in schizophrenia: from cognition to molecular pathways. Clinics (Sao Paulo). 66 (Suppl 1), 71–77. https://doi.org/10.1590/s1807-59322011001300009.

Youssofzadeh, V., Agler, W., Tenney, J.R., Kadis, D.S., 2018. Whole-brain MEG connectivity-based analyses reveals critical hubs in childhood absence epilepsy. Epilepsy Res. 145, 102–109. https://doi.org/10.1016/j.eplepsyres.2018.06.001.

Yu, Y., Shen, H., Zhang, H., Zeng, L.-L., Xue, Z., Hu, D., 2013. Functional connectivity-based signatures of schizophrenia revealed by multiclass pattern analysis of resting-state fMRI from schizophrenic patients and their healthy siblings. Biomed. Eng. Online 12, 10. https://doi.org/10.1186/1475-925X-12-10.

Zeev-Wolf, M., Levy, J., Jahshan, C., Peled, A., Levkovitz, Y., Grinshpoon, A., Goldstein, A., 2018. MEG resting-state oscillations and their relationship to clinical symptoms in schizophrenia. NeuroImage Clin. https://doi.org/10.1016/j.nicl.2018.09.007.